JOURNAL OF COMPUTATIONAL PHYSICS 66, 132–150 (1986)

Elements of a Computational Theory for Glaciers

S. YAKOWITZ

Department of Systems and Industrial Engineering, University of Arizona, Tucson, Arizona 85721

K. HUTTER

Laboratory of Hydraulics, Hydrology and Glaciology, ETH, Gloriastrasse 37–39, CH-8092, Zurich, Switzerland

AND

F. SZIDAROVSZKY

Department of Computer Sciences, University of Agriculture, H-1113 Budapest XI, Villanyi ut 29–35, Hungary

Received May 28, 1985; revised November 1, 1985

In recent years, theoretical glaciologists have derived a complete and highly credible model for ice masses. The model is based on standard conservation laws of physics as well as measured constitutive relations of ice. In this model, mechanical and thermal effects interact through nonlinear creep response laws, and the end product is a system of nonlinear partial differential equations with a free boundary condition. This model is easy enough to relate, but is probably intractible, analytically, and is far from trivial, computationally. This paper describes our strategy for solving a restricted, but nevertheless informative case: the uniaxial, cold, shallow, steady-state ice sheet with an idealized geometry. The authors believe that theirs is the first solution of the fully coupled equations. The details of a particular ice sheet computation are given, and qualitative implications are drawn. The computations go far toward settling some controversies in the glaciology literature, and bring to light questionable aspects of the "shallow ice" approximation.

1. INTRODUCTION

Recent years have witnessed the emergence of a reasonably complete thermomechanical theory for cold glaciers and ice sheets. This theory, stemming from important precursory work by Lliboutry, Nye, Weertman, and others (see citations in Paterson [30], or Hutter [15]) has found its most complete expression to date in studies by Fowler and Larson [7, 8, 9], Hutter and associates (Hutter [13, 14, 15], Hutter and Alts [16], Hutter and Vulliet [19], Hutter and others, [18]), and Morland and associates (Morland [27], Morland and Johnson [25, 26], Morland and Smith [27], Morland and others [28]). The ultimate goal

0021-9991/86 $3.00

is the determination of the temporal evolution of the ice sheet geometry and the associated temperature and velocity distributions. The theory is based on the fundamental physical laws of conservation of mass, momentum, and energy as well as constitutive relations summarizing laboratory experimentation on stress response behavior of isotropic polycrystalline ice. To these "field equations" are augmented some fairly indisputable boundary assumptions as well as somewhat disputable basal sliding laws. These ice mass equations turn out to couple thermal and mechanical effects through a rate function in the creep response law for stress, and the resulting model is a system of relatively formidable nonlinear partial differential equations which, to the best of our knowledge, is not subject to standard analytic solution techniques. Several authors (e.g., Morland and Smith [27]) have argued that the thermal component is significant: A model that does not couple the heat effects with the stresses is suspect.

There are a good many other computational glaciology studies in the literature. The closest in spirit to ours is Morland and Smith [27], who have computed the profile and ice fluid velocity of a steady-state ice sheet under the assumption that the temperatures are prescribed. There is another computational avenue which attempts to model ice masses with more realistic physical geometries based on actual measurement. Such realism has forced these investigators to use much more simplified models; such models have no pretense of being based entirely on laws of physics. A good example of this avenue is the study of the South Cascade Glacier in the state of Washington, reported by Hodge [11]. His two dimensional model only accounts for the flow velocities and height, the temperature field being taken as prescribed. Another idealization, following Nye [29], includes a shape-factor parameter, its role being to approximately account for the three dimensionality of the flow, as in Paterson [30]. Our estimation is that this and similar (e.g., Hooke *et al.* [12]) realistically inspired, physically simplified studies are valuable contributions to the computational attack on ice dynamics. When an inclusive computational methodology incorporating the strict physical modelling prescription of the present study is finally melded with finite-element procedures which, like Hodge's, can account for existing ice mass geometries, we will have come to a major milepost in theoretical glaciology. For the present, our inclinations are consonant with Fowler [6], p. 443], who says,

> In seeking the simplest realistic model of glacier flow, an attractive procedure is to analyse a given set of equations and boundary conditions in a mathematically consistent fashion, rather than make physically plausible, but nevertheless ad hoc, assumptions and approximations.

A companion paper [18] for an audience of research glaciologists stresses the modelling implications of our findings. We believe that together, these sister papers constitute a significant advance in the state of understanding of current glacier models. More generally, we hold that these sister papers constitute a fine example of the symbiosis of physical modelling and computation: The sophistication of the model required us to push to the forefront of computational practice. Computational discoveries forced us to consider important but nevertheless neglected

aspects and limitations of the widely accepted "shallow ice" approximation. We believe our results are significant and would have been unattainable without genuine interdisciplinary cooperation.

The plan of the paper is the following: Section 2 summarizes the Morland–Hutter model for a grounded, steady-state uniaxial ice sheet. The discretization of that partial differential equation model is described in Section 3, which elaborates on computational difficulties encountered, and our devices for overcoming them. Attention is given to numerical stability issues. Section 4 describes the results of a computational case study, and the concluding portion (Sect. 5) sketches ways in which we think our understanding of ice sheet dynamics has been enhanced by synthesis of physical and numerical analysis.

The vision which motivated our research effort is nicely encapsulated in an editorial introduction by Malcolm Mellor to Morland [23]. He states,

> Over the past few decades, understanding of the mechanics of ice and frozen soils has developed by piecemeal investigation of material properties, and by ad hoc application of conventional engineering mechanics to particular problems. Now, with increased motivations, resources, and basic knowledge, the time may be ripe for development of more general and rigorous theory and for greater professional involvement by applied mathematicians and theoretical mechanicians.

In the editorial following the above excerpt, Morland [23] noted that full solution had only been attained for temperature-independent ice response. We believe that our announcement (Yakowitz *et al.* [33]) and the present detailed study are the first to give a successful numerical procedure of the complete coupled thermomechanical free surface model.

Radok [31], in his *Scientific American* article on antartic ice, has described how new technology (radar and other remote sensing devices) has revolutionized ice sheet measurement. Toward the end of the article, he set the stage for the line of inquiry of the present paper by stressing that modelling efforts are needed to see how results of various studies "fit together to yield a comprehensive picture of East Antarctic ice and its environment." He observes the need for "models encompassing both the thermodynamics and dynamics of ice sheets," and notes that such models are the key toward scientific extrapolation regarding predictions of effect of antarctic ice on the global climate system and relevance to the "greenhouse effect," for instance.

In a more general vein, we are conscious that we are partaking of a fascinating historical moment, promised to us by Bellman, Ulam, Von Neumann, Wiener, and others, in which nonlinear modelling of complex systems is becoming feasible. Of course, the catalyst here is computer technology and methodology. For example, pleading in *Scientific American* for increased support for mathematical sciences, even on the basis of national self-interest, David [4] writes:

> One of the most promising current directions in fundamental mathematics is the continued development of the mathematical model. Mathematical modeling of natural phenomena is hardly new. Nevertheless, advances in numerical analysis and the development of the com-

> puter have made it possible to simulate processes in ways that are much more complex and more realistic than ever before. Mathematical modeling in partnership with the computer is rapidly becoming a third element of the scientific method co-equal with the more traditional elements of theory and experiment.

From examples offered in the above citations (weather prediction, nuclear winter, meteorology), one sees that hydroscience subjects are central, and understanding of ice masses will be a vital ingredient. Aside from its importance, glacier theory would seem to be a realm of fluid mechanics which is nicely suited to computer exploration, as we seek to show here.

2. The Ice Sheet Equations

Our computational aim in this paper is to "solve" a restrictive but nevertheless important subclass of Morland–Hutter models. The subclass we speak of is the two-dimensional steady-state cold shallow ice sheet. For simplicity in our exposition and calculations, we will assume that it lies on a flat plane, and that there is no basal drainage. However, such effects could easily have been incorporated. This model is significant in that it has also served as a starting point for other investigators working from first principles. For example, Morland and Smith [27] have used it to argue that the effect of temperature on the profile and velocity field is significant. To illustrate this point, they prescribe various plausible temperature patterns and solve the resulting (uncoupled) mechanical equations numerically. Fowler and Larson [8, 9] also prescribe temperatures in undertaking stability analysis of this model (with advection ignored) by "control space" tests and thereby conclude that the glacier differential equation model is stable. This approach avoids head-on numerical solution, but is not entirely conclusive. Their final paragraph is:

> Finally we remark that, of course, the inclusion of heat transport terms would lend the conclusion of this paper a great deal more authority. Such an inclusion, however, appears to render the problem almost intractable analytically, and numerical methods for such a double free boundary problem are beset with similar difficulties.

Morland [24] has set forth a very complete model with specific experimentally motivated choices for boundary conditions and for functions in the constitutive relations. We now relate these equations, giving only the scantiest justification and invite the reader to consult Morland [24] and Morland and Smith [27] for further details of the full derivation. The monograph by Hutter [15] also derives these equations (Chaps. 3 and 5), but does not offer specific choices of parameters and boundary conditions. On the other hand, Hutter's [15] derivation of the model is complete: The path from physical laws and laboratory measurements to the equations for ice masses is carefully marked out, as is the rationale behind the shallow ice approximation used in the Morland–Hutter models.

The setting for the equations is the Cartesian x–z plane with the transverse base of the glacier running in the x direction, and its height, at a particular position x,

being the position $H(x)$ in the z direction, as shown in Fig. 1. The dependent variables which we propose to approximate numerically are the internal temperature and internal horizontal, and vertical velocities, which are denoted by $T = T(x, z)$, $U = U(x, z)$, and $W = W(x, z)$, respectively. Also, we are to find the free surface profile $H(x)$. The field equations for these objects, all scaled appropriately and dimensionless, to the right of the ice divide, are:

Ice sheet differential equations.

$$U_z = a(T)\, g(\tau), \tag{2.1}$$

$$U_x = -W_z, \tag{2.2}$$

$$\beta T_{zz} = UT_x + WT_z - a(T)\, q(\tau). \tag{2.3}$$

Free surface differential equation.

$$UH' - W = A(x, H). \tag{2.4}$$

The stress $\tau = \tau(x, z)$ in (2.1) and (2.3) is determined by the free boundary height and slope according to

$$\tau(x, z) = -H'(x)(H(x) - z), \tag{2.5}$$

where here and elsewhere, the prime denotes the derivative of a univariable function.

We briefly discuss these equations. The first (Eq. (2.1)) is a constitutive relation, the "creep response law," $a(T)$ and $g(\tau)$ being laboratory-determined functions known respectively as the rate- and creep-response functions. The actual parameters of these functions, as prescribed by Morland [24] and Morland and Smith [27], are given in Table I. The second relation, (Eq. (2.2)), represents mass conservation under the assumption that ice is incompressible. Equation (2.3) for temperature is an energy balance relation. The second-order term on the left represents heat diffusion, the first order terms in T account for convection, and the final term represents internal energy dissipation. The prescribed constants β and the parametric functions $a(T)$ and $q(\tau)$ are offered in Table I. The constants α, β, and ε in that table are determined by the physical scales of a given ice sheet; for details see, our companion paper [18].

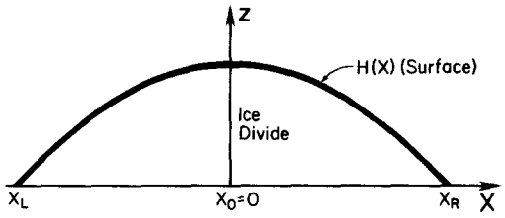

FIG. 1. Coordinates for uniaxial ice sheet model.

TABLE I

Functions and Parameters for Morland Realization of Ice Sheet Model

(a) Ice Sheet Functions

Rate function in (2.1)

$$a(T) = a_1 e^{b_1 T} + a_2 e^{b_2 T}$$

$$a_1 = 0.7242, \quad b_1 = 11.9567,$$

$$a_2 = 0.3438, \quad b_2 = 2.9494.$$

Creep response function in (2.1)

$$g(\tau) = 2\tau\omega(\theta\tau^2),$$

$$\omega(x) = 0.3336 + 0.3200x + 0.02963x^2.$$

Creep response function in (2.3)

$$q(\tau) = \alpha\tau g(\tau).$$

Accumulation function in (2.4)

$$A(x, H(x)) = \begin{cases} 12.5(H - H_e(x)), & H \leqslant H_e \\ 12.5(H - H_e(x)) - 76(H - H_e(x))^2 + 136(H - H_e(x))^3, & H_e \leqslant H < H_e + 0.25 \\ H_e(x), & H > H_e + 0.25, \end{cases}$$

where

$$H_e(x) = 0.5(1 - 0.1x).$$

Thermal flux in (2.7)

$$G(x) = 1.$$

Sliding law in (2.8)

$$u_F(H, H') = \frac{-\varepsilon^2 H'}{\mu_{\text{ref}} \tilde{\mu}(H)},$$

$$\tilde{\mu}(H) = \begin{cases} 9.0 - 6.657H(x), & 0 \leqslant H(x) \leqslant 0.7 \\ \sum_{j=0}^{5} \mu_j H(x)^j, & 0.7 \leqslant H(x) \leqslant 1.3 \\ 19.79 + 54.43(H(x) - 1.3), & H(x) > 1.3. \end{cases}$$

Surface temperature[a] *in* (2.9)

$$T_s(x, H(x)) = -0.1 - 0.5H(x).$$

(b) Ice Sheet Parameters[b]

$$\varepsilon^2 = 2.75 \cdot 10^{-6}, \quad \alpha = 0.5,$$

$$\theta = 9.01 \cdot 10^{-2}, \quad \beta = 0.02.$$

For sliding law

$$\mu_0 = -53.596, \quad \mu_3 = 26.753,$$

$$\mu_1 = 253.643, \quad \mu_4 = 176.028,$$

$$\mu_2 = -324.134, \quad \mu_5 = -72.761,$$

$$\mu_{\text{ref}} = 4.15 \cdot 10^{-8}.$$

[a] To obtain temperatures in centigrade, multiply by 20.

[b] The values for ε and θ are based on a stress scale of $10^5 P$, an accumulation rate of 1 m/yr, a typical stretching of 1 km/yr, a thickness of 2000 m, and an ice density of 918 kg/m^3.

The final relation (2.4) accounts for mass balance at the surface, and the function $A(x, H)$ gives the accumulation and ablation (net snow accumulation or melting of ice) at a given position and height. Morland and Smith's choice for this function is also given in Table I.

Our attention now turns to the boundary conditions.

A. *Basal Conditions*

The conditions at the bottom ($z = 0$) of the ice sheet are that there is no drainage, and the geothermal flux through the base is known. In equations, these two conditions are, respectively,

$$W(x, 0) = 0 \tag{2.6}$$

and

$$T_z(x, 0) = -G(x). \tag{2.7}$$

A sliding law relating slippage (high basal shearing) $U(x, 0)$ at the base to pressure gives a relation of the form

$$U(x, 0) = U_F(H(x), H'(x)), \tag{2.8}$$

Morland and Smith's [27] choice of parametric functions for G and U_F, and in fact all model parameters and specified functions are collected in Table I. The drag coefficient $\mu_{\text{REF}}\mu(H)$ was proposed by Morland, Smith, and Boulton [28] on the basis of Greenland ice sheet data. The value of μ_{REF} in Table I(b) is, however, smaller by a factor of about 100 than that suggested in [28]. By our choice, sliding becomes the dominant process. We were forced to make this modification in view of properties of the Morland–Hutter shallow ice model. Reasons will be given in Section 5.

B. *Free Surface Condition*

At the surface, we assume that the temperature is a prescribed function T_s of height and position. Thus at the surface

$$T(x, H(x)) = T_s(x, H(x)). \tag{2.9}$$

C. At the Ice Divide

Mathematically speaking, if the horizontal velocity $U(x, z)$ is continuous and, in the vicinities of the left and right extremes, flows towards these extremes, then there must be at least one continuous curve (not necessarily vertical), running from the base to the surface, along which the horizontal velocity U is zero. Such a curve is spoken of as an "ice divide." In our prototypical study here, for convenience and following Morland, we have assumed that the accumulation function $A(x, H)$ is

symmetric in x about $x=0$. This implies that the ice sheet is symmetric about 0, and the divide is at zero and is vertical. That is,

$$U(0, z)=0, \qquad 0 \leqslant z \leqslant H(0). \tag{2.10}$$

(This condition can also be shown to hold at the divide, regardless of symmetry, as a consequence of the shallow ice approximation). Furthermore, from symmetry follows the conclusion that at the divide, the surface slope must be zero:

$$H'(0)=0. \tag{2.11}$$

More can and must be said about conditions at the ice divide, because our computational strategy differs from that suggested by Morland [24] most significantly in that we use the ice divide as a boundary condition. (The reason for this variation is explained in the section to follow.) The gist of the situation is that to begin our computations at the ice divide, for any specified divide height $H=H(0)$, we must somehow find the temperature $T(0, z)$, the vertical velocity $W(0, z)$, and the second derivative $H''(0)$ of the surface at the divide. In view of (2.10), at the divide the model now becomes an ordinary two-point boundary value problem the one differential equation of which is

$$\beta T_{zz}=WT_z \tag{2.12a}$$

in the variables $T(0, z)$ and $W(0, z)$, with boundary conditions

$$\begin{aligned} T(0, H(0)) &= T_s(0, H(0)) \\ T_z(0, 0) &= -G(0), \\ W(0, 0) &= 0, \\ \text{and} \qquad & \\ W(0, H) &= -A(0, H) \end{aligned} \tag{2.12b}$$

Toward obtaining a second differential equation, note from (2.1) that

$$U(x, z)=U_F(H(x), H'(x))+\int_0^z g(\tau(x, z'))\, a(T(x, z'))\, dz'. \tag{2.13}$$

Differentiate this expression with respect to x and note that the incompressibility equation (2.2) gives us

$$\begin{aligned} U_x(0, z)=-W_z(0, z)=\int_0^z & [a(T(0, z'))\, g'(0)\, \tau_x\, dz' \\ & + [U_F(H(x), H'(x))]]_x|_{x=0}. \end{aligned} \tag{2.14}$$

In this conclusion, we have used that symmetry implies that $H'(0)$, and thus also the stress $\tau(0, z)$, defined in (2.5), must be zero, and any sensible creep function $g(\tau)$

such as Morland's, in Table I, must be zero when the stress is zero. In this fashion we conclude that $a'(T)\, T_x\, g(\tau)|_{x=0} = 0$. Now integrate (2.14) by parts, with respect to z, and use the surface condition (2.4), with $U(0, H) = 0$, to conclude that

$$A(0, H(0)) = -H''(0)\left[\int_0^H a(T)\, g'(0)(H-z)^2\, dz + \frac{\varepsilon^2}{\mu_{\text{REF}}\tilde{\mu}(H(0))}\right]. \tag{2.15}$$

From this expression, we obtain $H''(0)$, a term which will be required in our marching procedure. With (2.12a), (2.14), and (2.15), and boundary conditions (2.12b), we have all we need to find $T(0, z)$, $W(0, z)$, and $H''(0)$. This completes the specification of the boundary conditions at the divide.

D. *Steady-State Ice Mass*

The final condition required for the "steady-state" model is that the net accumulation be zero (or else mass conservation is defied). Mathematically, we thus have

$$\int_0^{x_R} A(x, H(x))\, dx = 0. \tag{2.16}$$

Values of the accumulation function $A(x, H)$ can be negative, to account for "ablation" (i.e., melting, calving, and perhaps, evaporation).

A careful derivation of the foregoing equations from first principles is given by Morland [24] and by our companion paper [18].

3. The Computational Strategy

This section reveals the details and properties of our specific numerical discretization of the ice sheet model. However, to motivate the technique, which might otherwise appear to have some arbitrary facets, some obstacles encountered in our investigation are first reviewed.

While containing no numerical results, Morland [24] outlined a plan of attack which we did find useful. However, he had reduced (2.16) to an equivalent end condition and proposed solving the problem by marching from the snout x_R. One may readily confirm that this entails solving the heat equation (2.3) in what amounts to the reverse time direction, a task known to be notoriously unstable, since the heat equation is irreversible in time. Our central contribution to this computational strategy is to propose solving by marching out from the divide $x = 0$. In this direction, the heat equation is stable. Since Morland's boundary conditions are symmetric in x about 0, solution of the equations in the region to the right of the ice

divide yields a complete description of the ice sheet. Our plan involves using the divide as a boundary condition, and marching in the direction of increasing x, until the surface meets the basal level, $z = 0$. It is perhaps useful to emphasize that this alternative computational idea does not involve any modelling assumptions beyond Morland's, but does entail squeezing as much information as possible from his model at the divide, as we have in point C of the preceding section.

Whereas we have spoken of "marching," it is clear that the ice sheet problem is in fact a boundary-value problem, and conditions at all domain points must be satisfied simultaneously. We account for this by regarding the height $H(0)$ at the divide as an unknown to be found, and by using what essentially amounts to a "shooting" method: For any fixed divide height H, the model (2.1)–(2.9), subject to all boundary conditions save (2.16), has a unique solution. We repeatedly calculate such solutions, iterating on the value of $H(0)$ until the net accumulation condition (2.16) is satisfied. When this happens, we have the ice sheet solution; all the boundary conditions are satisfied. The secant method (e.g., Szidarovszky and Yakowitz [32], Sect. 5.1]) was employed to direct iterations on $H(0)$; the function to be zeroed was the net accumulation value in (2.16), namely

$$F(H) = \int_0^{x_R(H)} A(x, H(x))\, dx. \tag{3.1}$$

In addition to the task of viewing the glacier model so that stable marching could be undertaken, another challenge appeared as soon as our computer code was tested; we should have anticipated this problem. We found that our estimates of the surface slope $H'(x)$, as computed from (2.4) oscillated wildly. A glance at this equation, which is equivalent to

$$H'(x) = \frac{W(x, H(x)) + A(x, H(x))}{U(x, H(x))}, \tag{3.2}$$

should have made us wary of subtractive cancellation error. Near the divide, the magnitudes of W and A agree to one or two significant places, and so discretization error alone can easily generate a relative error of $H'(x)$ on the order of several percent. A slight error here gets amplified at the next step, because in (2.1), $g(\tau)$ is very sensitive to $\tau = -H'(H - z)$. Yet computation of the surface slope was pivotal to our ice sheet marching strategy. The alternative to marching is simultaneous solution to some discretization of the ice sheet model, and this is undesirable because it involves solving a nonlinear equation of several hundred variables, and simultaneous solution is further complicated by lack of prior knowledge as to where the surface boundary $H(x)$ actually lies.

The device we employed to stabilize this calculation is a crude feedback control technique such as one might use to force some trajectory to follow a desired path in the presence of noisy measurements. The feedback technique uses as performance measure the difference between the actual and desired variable values, and adjusts

the control variable (in our case a single real number) according to whether or not the current measure is an improvement over the last iteration. In sensitive situations, one makes sure that the change at each stage is "moderate" to avoid overshoot, hunting, or outright loss of control.

In our case, in view of the surface boundary condition (2.4) the performance measure was naturally taken to be

$$\text{Fit}(x) = |H'(x) - (W(x, H(x)) + A(x,)H(x))/U(x, H(x))| \tag{3.3}$$

and at each step, $H'(x)$ is adjusted according to the rule

$$H'(x + \Delta x) = H'(x) + \Delta x H''(x),$$

where Δx is a discretization step size and

$$H''(x + \Delta x) = H''(x) \pm C\,\Delta x. \tag{3.4}$$

In (3.4), C is a fixed constant and the sign is chosen to be the same as that of the previous step if $\text{Fit}(x) < \text{Fit}(x - \Delta x)$. Otherwise the opposite sign is selected. The adaptive rule above seemed warranted because the direction of the effect of a change in H'' cannot always be predicted. The sign of the change of W/U with H' seems to depend on their relative magnitudes.

The feedback device just described appears to be sufficiently effective for our needs; for a wide range of ice sheet parameters, the function $\text{Fit}(x)$ is less than 0.05 throughout the computation, indicating that control was maintained. When the ice sheet parameters were held fixed, the computed temperature and velocity field, as well as the ice sheet profile, were not very sensitive to variations of the mesh dimensions Δx and Δz.

The Marching Algorithm

Presume the finite difference mesh step size Δx and Δz as well as the divide height $H(0)$ has been selected. Let $x(j) = j\,\Delta x$ and $z(k) = k\,\Delta z$. Terms like $T_{j,k}$ will be used to denote our estimates of T at positions $(x(j), z(k))$. It is reasonably apparent how the two-point boundary value problem (2.12a, 2.12b) for the ice divide temperature $T(0, z)$ and vertical velocity $W(0, z)$ may be solved. (We employed "quasilinearization" (e.g., Szidarovszky and Yakowitz [32]) to solve ordinary nonlinear finite difference two-point boundary value-problems such as is engendered by a discretization of the above equation, but readers will probably have their own favorite methodology). Once the solution is found, then a Riemann sum approximation of the integral in (2.15) will give us $H''(0)$. (Recall that $H'(0) = 0$ at the divide.)

Now we define the recursive marching step. Presume that for a fixed j, we have already computed H_j, H_j', H_j'', and $\{T_{j,k}, U_{j,k}, \text{ and } W_{j,k}\}$, $1 \leqslant k \leqslant N$, with $N = \text{int}(H_j/\Delta z)$. We give the recursion for finding the associated approximations at $j + 1$.

The symbol ∇ will denote the *divided* forward difference operator in the vertical direction: For any mesh function Q_{jk},

$$\nabla Q_{jk} = (Q_{j,k+1} - Q_{jk})/\Delta z.$$

The next surface height is given by

$$H_{j+1} = H_j + H'_j \, \Delta x. \tag{3.5}$$

For the temperature relation (2.3) and after approximating derivatives by the appropriate order of divided forward differences, we have

$$T_{j+1,k} = T_{j,k} + \frac{\Delta x}{U_{j,k}} [\beta \nabla^2 T_{j+1,k-1} - W_{j,k} \nabla T_{j+1,k} + a(T_{j+1,k}) \, q(\tau_{j+1,k})]. \tag{3.6}$$

This finite difference method is effectively the "backwards implicit approximation" for parabolic partial differential equations. It is known (e.g., Lapidus and Pinder [21, Sect. 4.5.2]) to be stable according to the Von Neumann criterion, regardless of mesh ratio $\Delta x/\Delta z$, for the linear heat equation. Other possible discretizations were not investigated. Equation (3.6) is subject to the boundary conditions (2.9) and (2.7), which we restate in discretized form:

$$T_{j,N} = T_S(x_j, H_j), \qquad \nabla T_{j+1,0} = -G(x(j+1)). \tag{3.7}$$

Quasilinearization served to solve this two-point boundary value difference equation in the independent variable k.

A Riemann sum approximation of U, in light of (2.1) is provided by the recursion

$$U_{j+1,k+1} = U_{j+1,k} + \Delta z \, a(T_{j+1,k}) \, g(\tau_{j+1,k}). \tag{3.8}$$

starting with $U_{j+1,0} = U_F(H_{j+1}, H'_{j+1})$. Once these horizontal velocities are known, (2.2) allows us to find the increments

$$W_{j+1,k} = W_{j+1,k-1} - \Delta z \cdot \nabla U_{j,k}, \tag{3.9}$$

and this, coupled with the boundary condition (2.6), restated as $W_{j+1,0} = 0$, yields all the vertical velocities at $j+1$.

The new $((j+1)$th column fit is calculated in terms of $U_{j+1,N}$, $W_{j+1,N}$, and $A(x(j+1), H_{j+1})$ from (3.3). Then H''_{j+1} is calculated as in (3.4) and attendant discussion.

This completes the detailed discussion of our numerical procedure. The marching halts when H_{j+1} reaches 0 (ground). The Riemann sum $\sum_j A(x(j), H_j) \Delta x$ approximation of the net mass term on the left side of condition (2.16) is accumulated as the calculations proceed and this constitutes the output of the procedure. The divide height $H(0)$ is adjusted according to the secant method until

this net accumulation is tolerably close to 0, as required by the zero mass flux condition (2.16).

Consistency and Convergence

We claim that the order of consistency, in the terminology of Meis and Marcowitz [22], e.g., is one, provided $\Delta z = O(\Delta x^2)$. Let us outline the basis for this claim. In brief, our marching procedure calculates temperature, velocities, and surface slope at the $(j+1)$th column in terms of data at the jth column. We must show that if we have given initial conditions $T(x, z)$, $H(x)$, $H'(x)$, $U(x, z)$, and $W(x, z)$ at $x = x(j)$, then the actual solution values $T(x_{j+1}, z_k)$ and $T_{j+1,k}$ their approximations obey the relation

$$\max_{1 \leqslant k \leqslant N} (|T_{j+1,k} - T(x_{j+1}, z_k)|) = O(\Delta x^2).$$

Further, $\mathbf{U}_{j+1} = \{U_{j+1,k}\}_{k=0}^{N}$ similarly has $O(\Delta x^2)$ local error. We have used here (and will use later) notation like $\boldsymbol{T}_j$ to denote the column vector $\{T_{j,k}\}_{k=0}^{N}$.

First, examine the temperature $\mathbf{T}_{j+1}$. Equation (3.6) takes the form

$$T_{j+1,k} = T_{j,k} + \Delta x F_k(\mathbf{T}_{j+1}; \mathbf{U}_j, \mathbf{W}_j, \mathbf{H}'_j, \mathbf{T}_j, H_j), \qquad 0 \leqslant k \leqslant N, \tag{3.10}$$

where the values $\mathbf{T}_{j+1}$ are computed so as to satisfy the linear two-point boundary value problem (3.6)–(3.7). The ideal coefficients depend on the unknown $\mathbf{U}_{j+1}$, $\mathbf{W}_{j+1}$, H'_{j+1}, and H_{j+1}, whereas we have used temperature, velocity, and surface data from the $x(j)$ column. But if these functions are twice-continuously differentiable, then the error so induced is $O(\Delta x)$, and from continuity results such as the comparison theorem in Birkhoff and Rota [2], we can anticipate this $O(\Delta x)$ error in difference equation coefficients to translate to $O(\Delta x)$ error in the computed solution $\mathbf{T}_{j+1}$ over a bounded domain. From these considerations, and the order of consistency demonstration in Meis and Marcowitz [22, p. 80] for the linear case, we have concluded that the order of consistency of the temperature is $O(\Delta x^2)$. This argument can be put a bit more forcefully by noting that in matrix notation, the backwards implicit parabolic difference equation takes the form

$$\mathbf{T}_{j+1} = \mathbf{T}_j + \Delta x\, \mathbf{Q}(\mathbf{T}_{j+1}, \mathbf{W}_{j+1}, \mathbf{U}_{j+1}, H_{j+1}, H'_{j+1})\, \mathbf{T}_{j+1}, \tag{3.11}$$

where the matrix $\mathbf{Q}$ absorbs the coefficients and inhomogeneous parts of the backwards implicit parabolic equation. This can be expressed as

$$\mathbf{T}_{j+1} = (\mathbf{I} - \Delta x\, \mathbf{Q}(\mathbf{T}_{j+1}, \mathbf{W}_{j+1}, \mathbf{U}_{j+1}, H_{j+1}, H'_{j+1}))^{-1} \mathbf{T}_j. \tag{3.12}$$

Now in our calculations, to avoid nonlinearity of the two-point boundary-value problem, we actually use $\mathbf{Q}(\mathbf{T}_j, \mathbf{W}_j, \mathbf{U}_j, H_j, H'_j)$ in place of the $\mathbf{Q}$ matrix function in (3.11). But the difference of these matrices is $O(\Delta x)$, which translates through the usual matrix perturbation relations (e.g., Szidarovszky and Yakowitz [32,

Sect. 6.3]) to an $O(\Delta x^2)$ perturbation in the solution $\mathbf{T}_{j+1}$. (The square stems from the observation that the Δx perturbation in Q itself gets multiplied by Δx in (3.12).)

The horizontal velocity $\mathbf{U}_{j+1}$ is updated according to (3.8), which is the rectangular quadrature formula (Davis and Rabinowitz [5]). It is readily established that under our differentiability assumptions, the rectangular rule global error is $O(\Delta z)$, which, recalling that $\Delta z = O(\Delta x^2)$, establishes that our error in $\mathbf{U}_{j+1}$ is $O(\Delta x^2)$. This term also reflects the dependency of $\mathbf{U}_{j+1}$ on the error in $\mathbf{T}_{j+1}$.

In computing $\mathbf{W}_{j+1}$ through (3.9), we loose an order in the error because of the Δx term in the denominator. Thus the local error of $\mathbf{W}_{j+1}$ equals $O(\Delta x)$. Finally, the error of H'_{j+1}, as computed from (2.4) must, in view of arithmetic perturbation relations (e.g., Szidarovszky and Yakowitz [32, p. 11]) be the minimum of the error orders of $\mathbf{U}_{j+1}$ and $\mathbf{W}_{j+1}$, namely 1.

Whereas the local errors of $\mathbf{T}_{j+1}$ and $\mathbf{U}_{j+1}$ are $O(\Delta x^2)$, and so satisfy the definition of consistency of order 1, the local error of $\mathbf{W}_{j+1}$ and H'_{j+1} has order 1. But this data propagates only through its effect on the Q matrix defined above, and in view of our earlier argument, we can stand $O(\Delta x)$ error here and still get $O(\Delta x^2)$ in the successive $\mathbf{T}$ and $\mathbf{U}$ vectors. This argument can be sharpened by referring to the Euler method for ordinary differential equations $\dot{x} = f(x)$. Here one solves

$$x_{n+1} = x_n + \Delta x f(x_n) + \Delta_n,$$

where Δ_n can collect all locally induced errors. In our case, $\Delta_n = O(\Delta x^2)$. From Theorem 8.1 of Szidarovszky and Yakowitz [32] (especially Eq. (8.19)), one sees that order 1 consistency and convergence will still be maintained.

In view of these facts, we claim that the order of consistency is 1, and under certain regularity assumptions, in view of the proof of the Lax–Richtmayer theorem (Meis and Markowitz [22, p. 62]) in the linear, constant coefficient case, one can hope that the order of convergence of the solution is likewise 1. We do not deny that certain delicate issues such as the nonlinearity of our equation in the face of the linearity requisite for the above convergence statement and the regularity needed in the discretization scheme have been glossed over here. A referee has noted that the structure of the ice sheet model somewhat resembles that of the Stefan problem of thermodynamics (e.g., Friedman [10, Chap. 8]). Thus perhaps more rigorous analysis along the lines of [20] is possible. Our asserted rate is the same as [20] derives for the Stefan problem.

4. A Numerical Solution to the Ice Sheet Model

The aim of this brief section is to lay claim to our being the first to provide a numerical solution to the full Morland–Hutter ice sheet model. The problem set forth in the preceding section is identical to that posed by Morland [24], with exception to the sliding law. This modification was necessary to conserve mass balance near the divide.

The specific problem functions and parameters were presented in Tables Ia and

Ib, respectively. We have found it more instructive to contemplate our solutions through (computer-generated) graphs than tables. Fig. 2 portrays the temperature field as well as the ice sheet profile. Pause to observe that throughout most of the ice sheet, the minimal temperature along vertical segments occurs in the interior. This and the occurrence of maximal temperatures near the base constitute a temperature inversion phenomenon which is known to exist in actual glaciers and ice sheets.

The computed velocity field is presented in Figs. 3 and 4. The curve denoted as (a) in Fig. 3 gives the net horizontal velocity, and the second (curve (b)) shows the "gliding velocity component. This is the difference between the horizontal velocities at the location indicated within the ice sheet and the basal velocity. The basal velocity is due to stress-induced sliding of the ice sheet over the bed. Evidently in this case, absolute values for velocities are large and only a small portion of the motion is due to the internal deformation of the ice. This stems from the small value of μ_{REF} used for this computation. Other more realistic situations do exist; the relevant analysis given in our companion paper [18] shows that by increasing basal drag, total velocities can be reduced and internal deformation then can contribute significantly to the total velocity. The no-slip condition cannot, however, be fully achieved within the shallow ice approximation, for reasons to be offered in Section 5. The final curve gives the velocity in the downward direction. Some had argued that near the snout (x_R), the vertical velocity might be upward due to melt. For here the accumulation is negative. Within the parameter ranges we investigated, the Morland–Hutter model seems clearly committed to saying that this velocity reversal does not necessarily occur: The slope H' and surface horizontal velocity in (2.4) are more than enough to balance negative accumulation.

Figure 4 plots the velocity field (horizontal and vertical components). To our eyes, the flow seemed consistent with common sense.

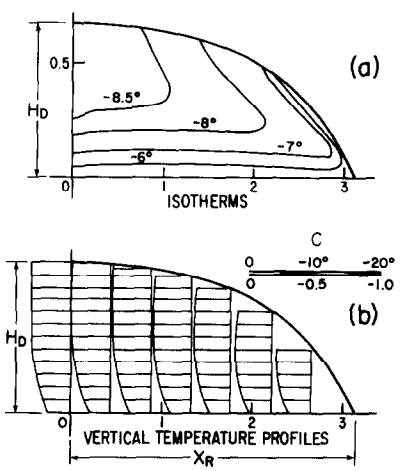

FIG. 2. Plots of isotherms and temperature profiles of the solution.

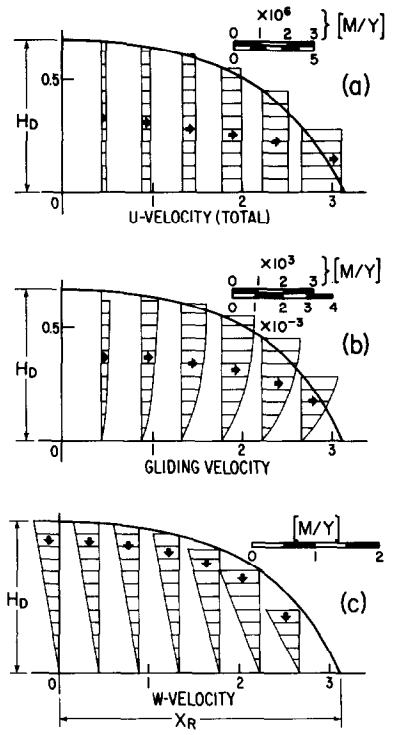

FIG. 3. Horizontal and vertical ice velocity profiles. Top of scales is in meters per year.

5. INTERACTIONS BETWEEN COMPUTATION AND MODELLING

Some of the implications of our methods and results with respect to theoretical glaciology will be outlined. Here our intention is only to argue that not only can we obtain specific solutions to specific problems, but in so doing, we uncover general

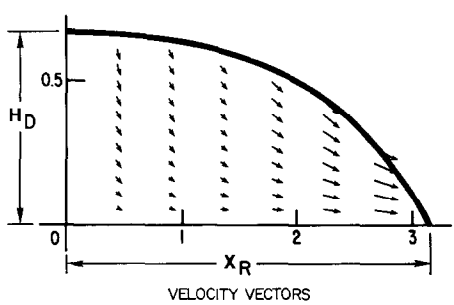

FIG. 4. Vector plot of the ice velocity.

strengths and weaknesses of current theoretical glacier models. In a sense, then, our studies involve interaction between modelling and computing. The glaciological motivations and conclusions are explained more fully in the companion study by Hutter *et al.* [18] intended for an audience of glaciologists.

Prior to our numerical studies of cold ice sheets under influence of external boundary conditions, our knowledge about the role and relative influence of the problem parameters and boundary conditions was inadequate. One had to be content with ad-hoc and plausibility arguments. We cite a few examples.

(1) While it was recognized that the accumulation rate function is the dominant factor determining the extent and geometry of the ice sheet, the role of temperature was only surmised. There was a question as to whether it had significant influence.

(2) Still with regard to the effect of temperature, it was clear that surface temperature and geothermal flux has a prime influence in determining the temperature field. The general nature of the effect of the diffusion term βT_{zz} and the vertical advection term WT_z in (2.3) could be anticipated (for reasons offered in Hutter [15, pp.170–174]). However, the influence of advection term UT_x in (2.3) and dissipation (the rightmost term in (2.3)) was difficult to anticipate from nonnumerical considerations.

(3) The significance of the sliding of the ice sheet on its bed relative to viscous deformation of the ice within the ice sheet was not even conjectured. It was anticipated that the creep phenomena are coupled in a complicated manner to the thermal field through the rate function $a(T)$ and the creep response functions $g(\tau)$ and $\omega(\theta\tau^2)$, so that the relative magnitudes of internal shearing and basal slip have effects which are hard to foresee.

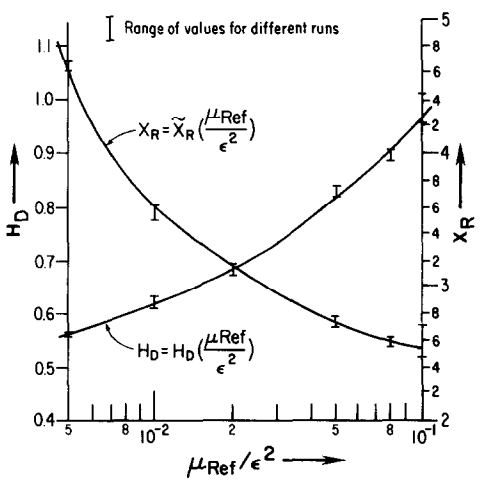

FIG. 5. Plot of ice sheet extents divide heights vs. sliding friction parameter.

To make a long story short, our computational approach, where we only set out to find the implications of the model, will end up forcing us and other glacier theoreticians to revise the model.

In the two subsections that follow, main qualitative conclusions reached from our study are outlined. These conclusions are among many, and they are offered here largely to illustrate the benefits of computational strategies to modeling of complex nonlinear systems.

Delineation of the Most Influential Ice Sheet Parameters

It was found by varying ε, θ, α, β, over glaciologically reasonable ranges that the ice sheet profile depended numerically on $\mu_{\text{ref}}/\varepsilon^2$ but, not significantly on α, β, and θ. Figure 5 shows this dependence. In this figure, error bars mark the range of values for x_R and H_D, respectively, which were obtained with different values of the parameters (more than 75 runs). The width of the error bars is more the reflection of the accuracy of our numerical computations than an indication of a dependence on other variables. To reach this conclusion we chose values for the ice parameters as follows:

$$\begin{aligned} &10^{-4} \leqslant \varepsilon \leqslant 10^{-1}, && 10^{-2} \leqslant \alpha \leqslant 1 \\ &10^{-4} \leqslant \theta \leqslant 10^{2}, && 10^{-2} \leqslant \beta \leqslant 5 \cdot 10^{-1} \\ &10^{-9} \leqslant \mu_{\text{ref}} \leqslant 10^{-5} \end{aligned} \tag{5.1}$$

and used the accumulation rate function of Table I.

In Fig. 5, we have plotted and interpolated heights $H(0)$ and extents x_R as functions of various values of $\mu_{\text{ref}}/\varepsilon^2$. As anticipated, the more "slippery" the base is, the more spread out the ice sheet will become.

Discovery of a Weakness of the Morland–Hutter Theory

By considering ranges of parameters thought physically possible, in Section 2 of the companion paper we established that necessarily

$$\frac{\mu_{\text{ref}}}{\varepsilon^2} < 0.2. \tag{5.2}$$

The surprising and distressing implication is that this allowable region of the ratio is smaller than glaciologists postulate. Physically, one would think that the "no slip" condition of $u_F \approx 0$ should be permissable. But this requires vastly larger values of $\mu_{\text{ref}}/\varepsilon^2$ (since u_F is proportional to the inverse of this quantity). This forces us to either reconsider what is reasonable, or push on to a different ice sheet model. Parenthetically we remark that the limitation (5.2) was only uncovered when we attempted numerical solution by marching from the divide. An obvious step along this latter path would be to discard the so-called "reduced model" which allowed

Hutter and Morland to pass from an elliptic to parabolic (with respect to x) heat equation for "shallow" ice sheets. The elliptic model at the divide has a stress term that could allow circumvention of (5.2).

ACKNOWLEDGMENT

This collaborative effort was supported by National Science Foundation Grant DPP-8219439: Numerical Solutions of Dynamical Problems Concerning Cold and Temperate Ice Sheets.

REFERENCES

1. G. BIRKHOFF, *SIAM Rev.* **25** (1), 1 (1983).
2. G. BIRKHOFF AND G. ROTA, *Ordinary Differential Equations* (Blaisdell, Waltham, MA, 1962).
3. D. CAMPBELL, J. CRUTCHFIELD, D. FARMER, AND E. JEN, *Comm Assoc. Comput. Mach.* **28**(4), 374 (1985).
4. E. E. DAVID, Sci. Amer. **252** (5), 45 (1985).
5. P. DAVIS AND P. RABINOWITZ, *Methods of Numerical Integration* (Academic Press, New York, 1975).
6. A. C. FOWLER, *J. Glaciol.* **24** (90), 443 (1979).
7. A. C. FOWLER AND D. LARSON, *Proc. Roy. Soc. London Ser. A*, **363**, 217 (1978).
8. A. C. FOWLER AND D. LARSON, *Geophys. J. Roy. Astron. Soc.* **63**, 333 (1980).
11. S. HODGE, *J. Glaciol.* (1986), in press.
12. R. HOOKE, C. RAYMOND, R. HOTCHKISS, AND R. GUSTAFSON, *J. Glaciol.* **24** (9), 131 (1979).
13. K. HUTTER, *J. Glaciol.* **25** (95), 29 (1981).
14. K. HUTTER, *Ann. Rev. Fluid Mech.* **14**, 87 (1982).
15. K. HUTTER, *Theoretical Glaciology* (Reidel, Dordrecht, 1983).
16. K. HUTTER AND T. ALTS, *Proc. XVI-IOTAM Congress on Theoretical and Applied Mechanics*, edited by F. I. Niordson and N. Olhoff (Elsevier Science, New York), p. 163 (1985).
17. K. HUTTER, F. LEGERER, AND U. SPRING, *J. Glaciol.* **27**, 224 (1981).
18. K. HUTTER, S. YAKOWITZ, AND F. SZIDAROVSZKY, *J. of Glaciol.* (1986), in press.
19. K. HUTTER AND L. VULLIET, *J. Thermal Stresses* **8**, 99.
20. J. W. JEROME AND M. E. ROSE, *Math. Comput.* **16** (160), 337 (1983).
21. L. LAPIDUS AND G. PINDER, *Numerical Solution of Partial Differential Equations in Science and Engineering* (Wiley, New York, 1982).
22. T. MEIS AND V. MARCOWITZ, *Numerical Solution of Partial Differential Equations* (Springer-Verlag, New York, 1981).
23. L. MORLAND, *Cold Region. Sci. Tech.* **6** 181 (1983).
24. L. W. MORLAND, *Geophs. Astrophys. Fluid Dynamics* **29**, 237 (1984).
25. L. W. MORLAND AND I. R. JOHNSON, Steady Motion of Ice, *J. Glaciol.* **25**, 229 (1980).
26. L. W. MORLAND AND I. R. JOHNSON, *J. Glaciol.* **28**, 72 (1982).
27. L. W. MORLAND AND G. D. SMITH, *J. Fluid Mech.* **140** 113 (1984).
28. L. W. MORLAND, G. D. SMITH AND G. S. BOULTON, *J. Glaciol.* (1984), in press.
29. J. F. NYE, *Geophys. J. Roy. Astron. Soc.* **4**, 431 (1963).
30. W. S. B. PATERSON, in *Dynamics of Snow and Ice Masses*, edited by S. C. Colbeck (Academic Press, New York/London/Toronto, 1980).
31. E. RADOK, *Sci. Amer.* 98 (1985).
32. F. SZIDAROVSZKY AND S. YAKOWITZ, *Principles and Procedures of Numerical Analysis* (Plenum, New York, 1978).
33. S. YAKOWITZ, K. HUTTER, AND F. SZIDAROVSZKY, *Z. Gletscherk.* **21**, 283 (1985).